Cobots for Covid: Modular Robot Design for Human Safety with Regard to Evolving Pandemics Phases

Jonathan Heidegger[1], Byung Wook Kim[1], Haoguang Yang[1], Mythra V. Balakuntala[1], Abigayle E. Moser[1,3], Shijie Zhu[2], Qizhong Li[2], Ali Doosttalab[1], Jhon J. Quiñones[1], Antonio Esquivel-Puentes[1], Tanya Purwar[1], Yu Chen[2], Hanyu Liu[2], Gangtie Zheng[2], Robin R. Murphy[5], Victor M. Castaño[4], Luciano Castillo[1], Nina Mahmoudian[1], and Richard M. Voyles[1]

[1] Purdue University, West Lafayette, IN 47907, USA,
{jheidegg, kim2986, yang1510, mbalakun, rvoyles}@purdue.edu
[2] Tsinghua University, Beijing 100084, China
[3] Iowa State University, Ames, IA 50011, USA
[4] Universidad Nacional Autonoma de Mexico, Coyoacan, 04510 Mexico City, Mexico
[5] Texas A&M University, College Station, TX 77843, USA

Abstract. This paper discusses the application of a modular collaborative robot designed to aid in the fight against COVID-19 in increasing safety for essential workers and students. We identify three main phases of a pandemic in onset, quarantine, and reopening which affect the demands and requirements placed on robots. The international team proposed a series of robotic modules that were deployed in hospitals, quarantine facilities, and classrooms, to be a telepresence for doctors, disinfects surfaces with UVC, disinfects air with a novel Bernoulli filter design, respectively. From these deployments we propose key benefits to a modular approach when designing robots for the current pandemic and future emergency responses.

1 Introduction

During the Ebola outbreak of 2014, robots were proposed as a logical technology for reducing risk to human caregivers. Despite the efforts of co-authors Voyles and Murphy and the White House Office of Science and Technology Policy [7][2], few thought robots were ready. Six years later, with the appearance of COVID-19, robots have blossomed onto the scene as a viable solution in many countries to protect humans from the spread of pandemic disease [20][24]. Throughout the COVID-19 pandemic, more than 200 different robots have been deployed for human safety [20] in every aspects, from the in-take of patients at emergency rooms to the monitoring of social distancing [26].

However, as the pandemic has progressed through three distinct phases we have identified: surge phase, quarantine phase, and re-opening phase, the needs for human protection have evolved, as well as the businesses and human populations most affected. The clinical, logistics, and educational sectors have all been

impacted by the phases of the COVID-19 pandemic [24]. In nearly every country, hospital workers were an obvious front-line concern as patient loads surged with the spread of the virus [25]. Robots became headline news [1] by enabling physical separation between sick people and vulnerable healthcare workers through remote teleoperation [26]. But as governments and societies practice quarantine policies, the term "essential workers" has generalized to include relatively low-paid cashiers and delivery personnel [21]. These workers, during the quarantine phase, were more numerous, harder to protect, with social contact with other people inevitable. Keeping a safe indoor environment for human interaction thus become top priority [18], where disinfection robots are involved [23][27]. Finally, the re-opening phase is characterized by enticing customers to return to businesses to help re-open the local economy. With the "essential worker" concept fading as the economy and social interaction revive, robots are required to work with non-worker humans around, which necessitates the adoption of "collaborative robots" (cobots) [12]. Specifically, education at both the university and K-12 levels became a hot-button topic [18] during the re-opening phase in the U.S.. Despite low levels of infections and symptoms among school-age children and teenagers, many students were reluctant to return to school. In light of this, we consider the education sector as a high-impact opportunity to address human-safe cleaning robots.

To be sure, these phases are not necessarily sequential nor are they orderly. Many regions experienced recurring and oscillating phases and thus shifts in needs. This shift in workplace needs has been a key obstacle to pandemic robot adoption. At Purdue, with clear need for the disinfection of empty rooms at the Purdue Village Quarantine Facility and full rooms of students – albeit, socially-distanced – in classes, a modular solution was preferred to spread development effort. As the main force in response to the pandemic shifts from hospitals to essential businesses, and further to schools and communities, the potential applications of robots increase [20]. While these robots service each fragmented application segments, they unveil critical challenges in keeping up with the shifting requirements during sporadic public safety events [17], [19]. Specifically, we deduced three main challenges from literature as:

1. Lack of cost and effort efficiency. The effectiveness of deployed robots in contrast to the cost and effort invested is low;
2. Lack of robot's adaptability to evolving situations and changing demands;
3. Lack of robot's readiness for similar future emergencies.

A potential solution to overcoming these challenges is to make robots modular. When responding to evolving low-incidence high-consequence events, such as the COVID-19 pandemic, modular robots are favored over application-specific robots due to their expansible capabilities - gained by swapping the functional modules [6]. This in turn presents advantages in operator familiarity, confidence in the systems, and reduced time and cost for emergency response [19], [9].

In response to the COVID-19 pandemic, our modular development and deployment of robots provide multi-modal services and unveil two key findings on modularity. Firstly, modularity reduces the effort to develop and deploy robots,

thereby allowing robots to fight a pandemic in the early stages and the following phases. Secondly, modularity decreases the cost needed to develop a robot that can adapt to requirements and demands to increase worker safety throughout all three phases of the pandemic.

2 Hardware Components

Our proposed modular design of the robot for COVID-19 response consists of five parts: a common omnidirectional mobile base, a Ultraviolet band-C (UVC) light disinfection module, an air filtration module, a medical care package, and a disinfectant spraying module, as shown in Fig. 1. The modules are added modularly onto the base to achieve multimodal disinfection and services, driven by specific application requirements. Specifically, the UVC and disinfectant spray apply to surface disinfection without occupants, and the Bernoulli air filtration module disinfects the indoor air to block transmission between occupants at their presence. In addition to the generic disinfection services, this robotic system is capable of hosting a medical care package that is speciallized to clinical care of the COVID-19 patients in quarantine. The dual-use of the robotic system circumvents rebuilding the entire robot for every specific scenarios, thus reduces the effort and cost of deployment and improves user familiarity.

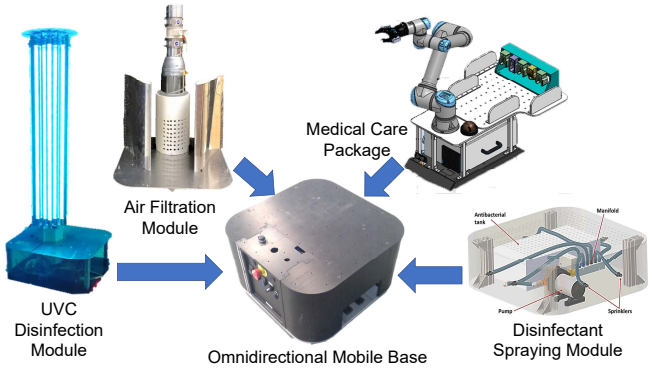

Fig. 1. Functional modules of the robot in response to the COVID-19 pandemics.

2.1 Holonomic Base as the Foundation of Mobility

For maneuvering the disinfection payloads, the robot consists of a common omnidirectional holonomic base with 4 powered caster wheels driven by 8 motors. The robotic base uses odometer and LiDAR sensors to support autonomous map navigation and dynamic obstacle avoidance in Robot Operating System (ROS) [27]. An operational space controller [13] overcomes overactuation, generating desired motion of the robot with decoupled three degrees of freedom,

and outputs wheel odometry as a byproduct. This foundation lowers constraints on path planning for modular designs such as a directional air filtration unit, or the direction agnostic UVC module. The choice to use the holonomic base which were already in use in other non-COVID projects, allowed for software and hardware to be developed modularly from a known interface and experience during the surge phase of the pandemic. The uniform software and hardware of the robotic system between different disinfection and operation types, enabled faster deployments thanks to the operator familiarity with the modules.

2.2 Bernoulli Air Filtration Module

When dealing with the reopening phase of the pandemic robotic solutions were looked for to aid in the protection of environments with people actively working or learning. The Bernoulli Air Filtration Module [27] is designed to reduce the number of Infections Bioaerosol droplets which range from 0.1 to 10 μm in diameter, which can suspend in air for hours, pose a major threat for horizontal transmission through inhalation when reopening. The Bernoulli module employs a novel design of air filtration system to increase the effectiveness of indoor air filtration when used with a mobile robot. The Bernoulli air filtration module brings medical-grade air treatment—a combination of particle filtration (a High Efficiency Particulate Air (HEPA) filter) and internal UV disinfection—to public indoor spaces, aiming to inactivate infectious bioaerosol droplets. Since the disinfection component is shielded and does not pose irritation to occupants, the module is suitable for disinfecting occupied indoor space, where transmission through air is a significant risk such as in classrooms and offices.

The filtration efficiency of the module, measured in percentage of the captured particles, is higher than 99.3% for particles larger than 0.3 μm, with capacity of 2.5 m^3/minute air. The flow tract design of the Bernoulli module, i.e. the AeroMINE™(Motionless, INtegrated Extraction) technology, originates from wind energy applications [14]. The filter design features low turbulance and large swept air volume to trap contaminants, facilitated by the motion of the filter when carried by the holonomic base. Using a pair of mirrored perforated airfoils and a perforated cylindrical tower, a low pressure zone is created between the airfoils which helps to drive the surrounding air into the intake of the system. The air is then driven by an axial fan in the cylinder through the HEPA filter, thus achieves high flow rate and efficiency, low turbulance air filtration.

2.3 UVC Disinfection Module

As infectious droplets are emitted by virus carriers, they start to precipitate onto surfaces, which causes surface contamination and therefore poses risk of community spread. As a result, regular surface disinfection is required by pandemic prevention regulations, which calls for a direct method of killing the pathogen on surfaces. The UVC with wavelength of 254 nm is proven to be germicidal [16], and has been applied in hospitals. However, UVC is also harmful for humans under direct exposure [10], which necessitates the automation of unattended

UVC disinfection process through robots. The proposed UVC disinfection module consists of eight mercury vapor bulbs installed on a tower for illuminating the surrounding walls and floors, 360 degrees around. A stop-and-move scheme is adopted for the robot, to apply illumination dosage more uniformly around the target facility. The surface dosage at a certain indoor spot is thus achieved based on the location of each stopping location of the robot and their corresponding dwell times, as illustrated in Section 3.1.

2.4 Disinfectant Spraying Module

Spraying disinfectants is a hospital-proven measure of epidemic prevention [22]. However, since it is a labor-intensive job performed by staffs, and disinfectants usually cause some form of irritation to human body, and the contaminated surfaces poses risks of infections, the staffs are exposed to two-fold hazard risks without extensive protection. We therefore propose a novel nanoparticle disinfectant solution and micro-spray system that, when combined with an autonomous mobile robotic base, can run either pre-scheduled or teleoperated.

The module features a three gallon tank containing antimicrobial solution. The nozzles system features a diaphragm pump connected to a manifold to split the flow into several nozzles, to produce a disinfectant cone-shaped mist with an average droplets size of $\sim 50\,\mu$m. The micro-droplet cloud from the nozzle can cover a radius of up to 2.25 m in the surrounding area of the robot. To enhance coverage in corners and hard-to-reach areas, an Electrostatic Spray Deposition (ESD) unit is also added.

2.5 Medical Care Module

The medical care module consists of a Universal Robots UR5 arm and a suite of tools for assessing the health of patients. The considered health assessment tasks of the medical care module are taking body temperature, operating the stethoscope, and ultrasound diagnosis, since they cover the common symptoms used in infection screening (fever, coughing, etc.), and provides valuable observations of the patient's organs. As a result, an infrared thermometer, a electronic stethoscope, and an ultrasound probe are included as end-effector tools of the robotic arm. The tools are mounted on 3D-printed adapters to suit the grabbing gesture of the gripper on the robotic arm, and stored in a toolbox for on-demand access of the arm. The module is also equipped with a speaker and microphone for two-way audio communication.

The tools, when attached to the robotic arm, are associated with their different interaction dynamics. The temperature taking task is contact-free, therefore a visual-servoing approach is adopted to pinpoint the tool with respect to the face of the patient. The stethoscope involves point-wise contact to the patient, while the ultrasound probe involves contact with sliding and gimbaling. Both the stethoscope and ultrasonic examinations require a certain amount of contact force between the probe and the skin of the patient, considering the reception

quality. To accomplish this while ensuring patient safety, a contact force controller is developed to relieve operator burden and prevent patient discomfort. The controller limits the normal force applied at the probe, through measurements from the wrist force sensor on the robotic arm.

3 Software Components

In support the the modules there is also extensive work to develop modular software to meet the demands of the rapidly changing pandemic. The robots share software and with module specific software developed in individual software tasks subroutines. Unifying the modules is the teleoperation modules which must work with the robot base and provide users access to module specific functions.

3.1 Planning objectives of the UVC module

When determining the desired path for the UVC equipped robots we employ simulations to verify the paths effectiveness and plan more optimal paths. The UCV disinfection paths are simulated in Matlab using a ray casting approach to determine sample points on the map to accumulate UVC dosage. This dosage was calculated based on dwell time and UVC power at different distances, which is a 2D simplification of the method discussed in [8]. We gathered experimental data from 8 different points ranging from 10cm to 120cm to produce a exponential function, as shown in Fig. 2(a) to inform UVC lamp dosage. As a reference, surface dosages over 50mJ/cm2 is shown to effectively kill the SARS-CoV-2 virus [5].

Once a path has been verified in Matlab a combination of a UVC Dosimeter and UVC dosage stickers are used to corroborate the simulation. This simulation is limited to 2-D due to two considerations. Firstly, the UVC bulbs are fixed vertically to a tall tower, which promotes uniform exposure on all vertical surfaces. Secondly, the simplicity of 2-D estimates vastly increases the speed of deployment to verify paths without having to expend on site time to test paths which average an hour to complete per path.

3.2 Planning objectives of the Bernoulli Air Filtration Module

A similar approach is being considered with the air filtration robot with applying experimentally gathered particle count data with Computational Fluid Dynamics (CFD) analysis done of a classroom to identify hot spots for the robot to clean. We assume identical spreading pattern of the infectious bioaerosol emitted from each individual occupant. The individual spreading pattern is computed using CFD with a simulated mouth and airflow speed and droplet diameter profile of a cough obtained from [11]. Upon a room with multiple occupants, the spreading of bioaerosol particles from each individual is superimposed as a simplification to circumvent computational-intensive calculation of the CFD, which is infeasible for on-site evaluation. Then, a modified convection-diffusion model [27] is

Distance (cm)	UVC Dosage (μW/cm^2)
38.1	497
71.1	296
125.7	121
186.7	72
247.7	46
308.6	32

(a)

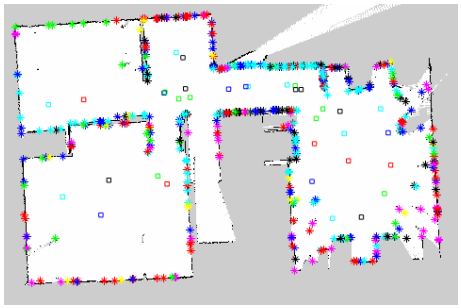

(b)

Fig. 2. (a) UVC dosage measured at various distances and same height level from the module. (b) A result of a simulated UVC disinfection where stars are representative of accumulation points and squares are the robot path points. Accumulation points are color coded based on UVC dosage (Red: <45, Yellow: <50, Green: <60, black: <100, cyan: >100. Unit: mJ/cm^2).

applied to estimate the effect of the air filter on the spread of the particles. The path of the robot during the air filtration task is parameterized by the frontal passing distance and speed of the robot in front of each occupant. The parameters are optimized based on the simulation result to minimize the cumulative particle weights inhaled by each occupant, should one of their neighbors cough.

3.3 Unified Teleoperation User Interface

Although the robot involves certain degree of autonomy in navigation and motion planning, the versatile nature of application scenarios means that a one-fits-all solution does not exist. To move the robot around reliably in all scenarios of interest, a teleoperation interface is thus required for when full autonomous navigation is not well suited such as in unstructured environments. To enhance operator familiarity, the teleoperation interface adopts unified, intuitive, and user-friendly input devices, consisting of a 3-DoF joystick and an optional 6-DoF space mouse. The planar motion of the robotic base is directly controlled by the 3-DoF joystick, while the robotic arm of the medical care module can be controlled by either the joystick (by remapping) or the space mouse, depending on the user preference. Visual feedback is the most intuitive approach to notify the operator about the surroundings of and troubles encountered by the robot. As a result, a frontal chassis camera is set on the robotic base, and an eye-in-hand camera is embedded on the robotic arm facing the gripper (on the medical care module) for the operator to gain situational awareness and monitor robot motion.

Concerning operator workload, network latency and bandwidth limits, the teleoperation approach is an augmentation, rather than substitution, of the existing autonomy. While teleoperation is required for contact-based medical tasks such as ultrasound and stethoscope operations, it is an on-demand component

that augments other automated tasks the robot is capable of. For instance, the robot may need human assistance to recover itself when navigating in confined door thresholds or classrooms, which the on-board path planner is not well optimized for. Given that the robot can still achieve autonomous navigation except in scattered edge cases, a small effort in teleoperation as error correction can widely expand the applicability of the robot.

To make the robot learn from these error correction events, such that human intervention can be further reduced, a model-free learning from demonstration (LFD) framework is proposed [3]. The framework eliminates explicit reward engineering by inferring the reward from the goal states collected from expert demonstrations of the skill. Robot states from the demonstration are extracted to correlate with the success/fail result of the teleoperation. The extracted states are then used to train a classifier which ultimately represents the reward. To accelerate the learning process such that fewer demonstrations are needed before the model converges, a one-shot learning scheme is adopted with further corrections made through coaching. Using a decision tree classifier, the demonstration is semantically segmented into a sequence of actions the robot can perform (via points in this case). The skill parameters are then updated using a self evaluator based on the execution performance to ultimately improve the task performance, thereby locally optimizing cumulative performance [4]. As a result, the LFD framework allows the modular robot to learn ways to overcome unexpected situations from few demonstrations.

3.4 Fleet management

To manage the fleet of robots and monitor their running status, the robot statuses are uploaded onto a centralized database. Each robot transmit four types of information – telemetry, base navigation, motor status, and payload status. These information helps assistance team assess the health status of the robot and determine if maintenance is required. To ease up the inspection of these data, an IoT web dashboard is created using Grafana software. The dashboard provides graphical interface of the historical data that each robot transmitted and sends out alerts through web-hooks when values are abnormal.

4 Deployments and Experiments

To validate the individual modules and the integration of modules, a series of deployments were done in a variety of settings in both the quarantine and reopening phase. Through these deployments, data is gathered to measure the efficacy of individual modules and to gain key insights to improve designs for the future.

4.1 Medical Care Package at Beijing and Wuhan hospitals

To prove the effectiveness of the medical care module, experiments were conducted in hospitals in Wuhan Union Hospital and Beijing Ditan Hospital, as

shown in Fig. 3. These locations were overwhelmed with SARS-CoV-2 patients during the surge and quarantine phases. The robot assisted the doctor in diagnosing patients with the help of an on-site nurse. Using our system, the doctor can chat with the patient as well as see the real-time result of the ultrasound examination remotely. The real-time sound of the patient breathing was picked up by the electrical stethoscope and transmitted to the the doctor. The digitized data was recorded by the doctor for future analysis.

Fig. 3. The Medical Care Module during a trial in Beijing Ditan hospital. The robot was performing ultrasound diagnosis through augmented teleoperation. The monitor is set up for the assistant nurse, who applies the ultrasound gel, and takes over the robot with a radio control in case of emergency.

A survey was distributed to physicians that participated in the training for robot operation and medical trials, and four valid responses were collected. The survey features subjective evaluations that compares the users' experience with the robot as a telepresence device versus the absence of the robot. The survey evaluates the benefits of the robot when using different input devices for different functions or purposes. The result of the survey is averaged and summarized in Table 1. According to the survey, despite the unified input interface for teleoperation, the operator familiarity and user experience is still negatively related to the complexity of the task. Although the robot physically separates the medical staff from the patients, the ease of use of the robot still needs to be improved.

4.2 UVC module at the Purdue Quarantine Facility

The UVC module has been tested in the quarantine facility at Purdue University. Using the simulations outlined in 3.1 a disinfection path was chosen that complied with reachability and necessary dosage. The paths were verified within the quarantine facility using a combination of an electronic UVC dosimeter and UVC Dosage cards to verify a minimum dosage of 50 mJ/cm2. to corroborate the data collected a deployment with T1 Phage samples placed throughout the room was conducted in a method similar to [15]. With 4 test sites and a control kept in full occlusion we were able to demonstrate an effective cleaning of the room. We can see that in 2 there is an approximately 3 log reduction in phage concentration even in challenging locations with complex shadows such as a gap

Table 1. Result of the survey on user experience with the robot with medical care module. Items are scored on a 0 – 100 scale, where 0 stands for poor/totally disagree, and 100 stands for good/totally agree.

Items		Scores
Robot ease of control	robotic arm	67.25
	mobile platform	63.25
Human-machine interface	3DoF joystick	56
	6DoF space mouse	53.75
Likelihood of using the robot compared to in-person operation	temperature taking	88
	stethoscope	79.5
	ultrasound	54.25
Reasons contributing to the use of robots	remote operation	91
	improved efficiency	54
	better patient experience	46.75

between the fridge and cabinets (Location 3). The robotic disinfection is effective and takes less time than static UVC that has been used before [16].

Table 2. Testing UVC illumination effectiveness with T1 phage in culturing broth. Two drops of 5μL T1 broth are placed on a microscope slide cover at each location. After irradiation, place the cover glass into 10 mL tryptic soy broth (TSB) for virus extraction. Log reduction is calculated via a comparison to the control.

Sample	Concentration (PFU/mL)	Log Reduction	UVC Dosimeter Card Reading (mJ/cm^2)
Onsite control	5.12E+06		
Location 1	1.42E+02	-4.56	128.38
Location 2	1.26E+03	-3.61	132
Location 3	1.04E+04	-2.69	73.53
Location 4	5.22E+02	-3.99	109.53

The actual position of the robot during the UVC disinfection run is recorded in the database, which is later retrieved for validation of the actual dosage. The verification uses the same dosage estimation software as shown in Fig. 2(b), which reveals the underexposure locations due to variations in localization and obstacle positions. The indication of underexposure will guide janitorial staffs for the follow-up spot-cleaning.

4.3 Bernoulli Air Filtration module in Purdue Classrooms

To explore the effectiveness of the Bernoulli robot, experiments within a real classroom setting is carried out as shown in Fig. 4. The purpose of the experiment is to show that (a) airborne particles created by human activities are local to the people's locations, and (b) the motion of the robot does not excite excessive amount of sedimented particles (such that the combination of robotic base with

the air filtration module yields net decrease of airborne particles). As a result, the robot is set to move in a serpentine pattern that passes in front of every occupant as suggested in [27]. Two particle counters (VPC300) are placed on the robot to measure the particle concentration around the robot and its spatial variation. For comparison, two sets of measurements were made – one with the air filtration module powered on, and one without.

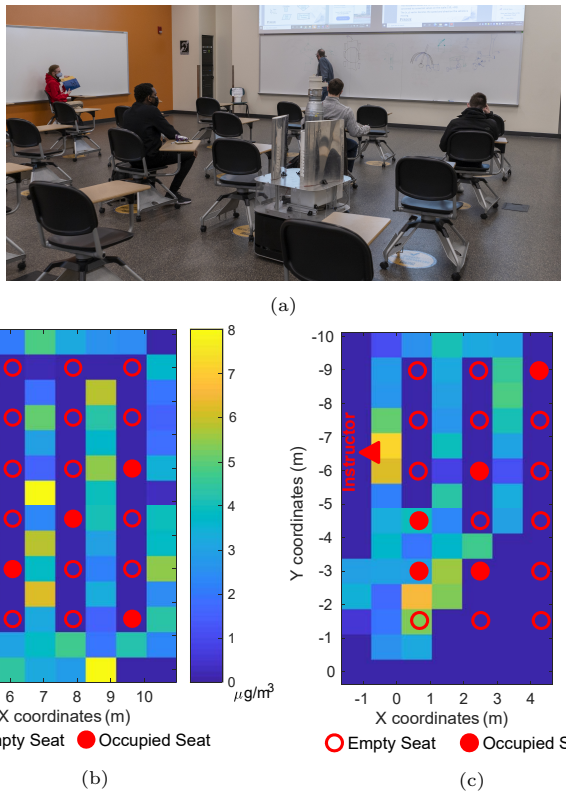

Fig. 4. (a) Testing the robot with air filtration module in a classroom. (b) Particle concentration map with air filtration off. (c) Particle concentration map with air filtration on.

The measurements from the particle counter are labeled with time, which is correlated with the localization logging of the robot stored on the database. The dosage measurement at discrete locations are then cast and averaged on a grid division of the working area, such that the size of a grid roughly equals to the distance traveled of the robot during a sampling window. Since a larger particle has the capacity of carrying more contaminant, the particle counts at each diameter channel are weighted by their volumes and summed together. The density of the particles are assumed to be the density of water, which yields

the measuring unit of particle concentration being $\mu g/m^3$. The concentration map of the two experiments are shown in Fig. 4b, c. From the concentration map, whether a seat is occupied strongly correlates ($p = 0.003$) with the particle count nearby, which indicates that the airborne particles created by human activities has locality as long as the occupants remain stationary. By comparing the particle counts without and with air filtration, the maximum particle count (grid-averaged) has reduced from $27.01\,\mu g/m^3$ to $12.75\,\mu g/m^3$, while the time-averaged particle count has reduced from $3.66\,\mu g/m^3$ to $3.47\,\mu g/m^3$. This result confirms the effectiveness of the module.

5 Conclusion

During this pandemic we have seen the effects of increased robotic deployment towards the COVID-19 crisis. As the pandemic evolved, different industries made unique demands and induced application-specific robots to be developed. However, the deployed robots - designed for a single purpose - face several limitations such as lacking efficiency, adaptability and future readiness. We address the inefficiency and inflexibility issues by introducing modularity, thereby allowing a single robot to have several different purposes and functions instead of one. The modular robot we developed works by attaching and detaching "modules" from a universal mobile base depending on the task the robot has to complete. From ultrasound and stethoscope measurements to UVC disinfection and air filtration, our modular robot can execute risky tasks without endangering the lives of workers. We evaluated the overall performance for a variety of settings when each module is attached to the uniform navigation base. The successful navigation of the robot using a single mobile base and a unified software illustrates the effort efficient manner of our approach. For every different module test, we didn't have to completely reprogram the robot. In addition, results of the individual module experiments show the effectiveness of task execution. Notably, the air filtration module reduced maximum particle count from $27.01\,\mu g/m^3$ to $12.75\,\mu g/m^3$. In the future, this framework can be extended to incorporate more complex procedures and implement learning from demonstration frameworks, ultimately providing the robot with more flexibility and increased semi-operability.

6 Acknowledgements

This work was funded in part by Tsinghua University, Intel Corp Covid-19 fund, the Indiana Manufacturing Institute, the NSF RoSe-HuB Center, and NSF under CNS-1439717.

References

1. 10 ways robots fight against the covid-19 pandemic (2020). URL `https://www.eu-robotics.net/eurobotics/newsroom/press/robots-against-covid-19.html`

2. Ackerman, E.: Real robots to help fight ebola. IEEE Spectrum (2014). URL https://spectrum.ieee.org/automaton/robotics/medical-robots/real-robots-to-help-fight-ebola
3. Balakuntala, M.V., Kaur, U., Ma, X., Wachs, J., Voyles, R.M.: Learning multimodal contact-rich skills from demonstrations without reward engineering. In: IEEE International Conference on Robotics and Automation (ICRA)) (2021). URL https://arxiv.org/abs/22103.01296
4. Balakuntala, M.V., Venkatesh, V.L.N., Bindu, J.P., Voyles, R.M., Wachs, J.: Extending policy from one-shot learning through coaching. In: 2019 28th IEEE International Conference on Robot and Human Interactive Communication (RO-MAN), pp. 1–7 (2019). DOI 10.1109/RO-MAN46459.2019.8956364
5. Biasin, M., Bianco, A., Pareschi, G., Cavalleri, A., Cavatorta, C., Fenizia, C., Galli, P., Lessio, L., Lualdi, M., Tombetti, E., Ambrosi, A., Redaelli, E.M.A., Saulle, I., Trabattoni, D., Zanutta, A., Clerici, M.: Uv-c irradiation is highly effective in inactivating sars-cov-2 replication. Scientific Reports **11**(1), 6260 (2021). DOI 10.1038/s41598-021-85425-w. URL https://doi.org/10.1038/s41598-021-85425-w
6. Brunete, A., Ranganath, A., Segovia, S., de Frutos, J.P., Hernando, M., Gambao, E.: Current trends in reconfigurable modular robots design. International Journal of Advanced Robotic Systems **14**(3), 1729881417710,457 (2017). DOI 10.1177/1729881417710457. URL https://doi.org/10.1177/1729881417710457
7. Bryant, R.: Innovating to fight ebola (2014). URL https://obamawhitehouse.archives.gov/blog/2014/11/17/exploring-opportunities-robotics-aid-disease-outbreaks. Retrieved on Apr 26, 2021
8. Conte, D., Leamy, S., Furukawa, T.: Design and map-based teleoperation of a robot for disinfection of covid-19 in complex indoor environments. In: 2020 IEEE International Symposium on Safety, Security, and Rescue Robotics (SSRR), pp. 276–282 (2020). DOI 10.1109/SSRR50563.2020.9292625
9. Di Lallo, A., Murphy, R., Krieger, A., Zhu, J., Taylor, R.H., Su, H.: Medical robots for infectious diseases: Lessons and challenges from the covid-19 pandemic. IEEE Robotics & Automation Magazine **28**(1), 18–27 (2021). DOI 10.1109/MRA.2020.3045671
10. FDA: UV lights and lamps: Ultraviolet-c radiation, disinfection, and coronavirus (2021). URL https://www.fda.gov/medical-devices/coronavirus-covid-19-and-medical-devices/uv-lights-and-lamps-ultraviolet-c-radiation-disinfection-and-coronavirus
11. Gupta, J., Lin, C.H., Chen, Q.: Flow dynamics and characterization of a cough. Indoor air **19**(6), 517–525 (2009)
12. Holland, J., Kingston, L., McCarthy, C., Armstrong, E., O'Dwyer, P., Merz, F., McConnell, M.: Service Robots in the Healthcare Sector. ROBOTICS **10**(1) (2021). DOI {10.3390/robotics10010047}
13. Holmberg, R., Khatib, O.: Development and control of a holonomic mobile robot for mobile manipulation tasks. The International Journal of Robotics Research **19**(11), 1066–1074 (2000). DOI 10.1177/02783640022067977
14. Houchens, B.C., Marian, D.V., Pol, S., Westergaard, C.H.: A novel energy-conversion device for wind and hydrokinetic applications. In: Fluids Engineering Division Summer Meeting, vol. 59070, p. V004T04A013. American Society of Mechanical Engineers (2019)
15. Jelden, K.C., Gibbs, S.G., Smith, P.W., Hewlett, A.L., Iwen, P.C., Schmid, K.K., Lowe, J.J.: Ultraviolet (uv)-reflective paint with ultraviolet germicidal irradiation

(uvgi) improves decontamination of nosocomial bacteria on hospital room surfaces. Journal of Occupational and Environmental Hygiene **14**(6), 456–460 (2017). DOI 10.1080/15459624.2017.1296231. PMID: 28278065
16. Lindblad, M., Tano, E., Lindahl, C., Huss, F.: Ultraviolet-c decontamination of a hospital room: Amount of uv light needed. Burns **46**(4), 842–849 (2020). DOI https://doi.org/10.1016/j.burns.2019.10.004
17. Malik, A.A.: Robots and covid-19: Challenges in integrating robots for collaborative automation (2020)
18. Morawska, L., Milton, D.K.: It Is Time to Address Airborne Transmission of Coronavirus Disease 2019 (COVID-19). Clinical Infectious Diseases **71**(9), 2311–2313 (2020). DOI 10.1093/cid/ciaa939. URL `https://doi.org/10.1093/cid/ciaa939`
19. Murphy, R.R., Adams, J., Gandudi, V.B.M.: Robots are playing many roles in the coronavirus crisis – and offering lessons for future disasters (2020). URL `https://theconversation.com/robots-are-playing-many-roles-in-the\-coronavirus-crisis-and-offering-lessons-for-future-disasters-135527`. Retrieved on Mar 29, 2021
20. Murphy, R.R., Gandudi, V.B.M., Amin, T., Clendenin, A., Moats, J.: An analysis of international use of robots for covid-19 (2021)
21. Office, D., OECD: The impact of the covid-19 pandemic on jobs and incomes in g20 economies (2020). URL `https://www.ilo.org/global/about-the-ilo/how-the-ilo-works/multilateral-system/g20/reports/WCMS_756331/lang--en/index.htm`
22. Otter, J., Yezli, S., Perl, T.M., Barbut, F., French, G.: The role of 'no-touch'automated room disinfection systems in infection prevention and control. Journal of Hospital Infection **83**(1), 1–13 (2013)
23. Potenza, A., Kiselev, A., Saffiotti, A., Loutfi, A.: An open-source modular robotic system for telepresence and remote disinfection (2021)
24. Shen, Y., Guo, D., Long, F., Mateos, L.A., Ding, H., Xiu, Z., Hellman, R.B., King, A., Chen, S., Zhang, C., Tan, H.: Robots under covid-19 pandemic: A comprehensive survey. IEEE Access **9**, 1590–1615 (2021). DOI 10.1109/ACCESS.2020.3045792
25. WHO: Keep health workers safe to keep patients safe (2020). URL `https://www.who.int/news/item/17-09-2020-keep-health-workers-safe\-to-keep-patients-safe-who`. Retrieved on Mar 29, 2021
26. Yang, G.Z., J. Nelson, B., Murphy, R.R., Choset, H., Christensen, H., H. Collins, S., Dario, P., Goldberg, K., Ikuta, K., Jacobstein, N., Kragic, D., Taylor, R.H., McNutt, M.: Combating covid-19 – the role of robotics in managing public health and infectious diseases. Science Robotics **5**(40) (2020). DOI 10.1126/scirobotics.abb5589
27. Yang, H., Balakuntala, M.V., Moser, A.E., Quiñones, J.J., Doosttalab, A., Esquivel-Puentes, A., Purwar, T., Castillo, L., Mahmoudian, N., Voyles, R.M.: Enhancing safety of students with mobile air filtration during school reopening from covid-19. In: 2021 IEEE International Conference on Robotics and Automation (ICRA) (2021). URL `https://arxiv.org/abs/2104.14418`